

Moving mirrors, Page curves and bulk entropies in AdS₂.

Ignacio A. Reyes^{1,*}

¹*Max-Planck-Institut für Gravitationsphysik, Am Mühlenberg 1, 14476 Potsdam, Germany*

(Dated: March 3, 2021)

Understanding the entanglement of radiation in QFT has been a long standing challenge in high energy physics, with implications ranging from black hole thermodynamics to quantum information. Progress has been traditionally limited to consideration of either universal quantities fixed by symmetries, or global properties of the asymptotic states. Here we demonstrate how the free fermion in 1 + 1 dimensions allows to go beyond by revealing the details of the density matrix of the radiation produced by a moving mirror, that in general breaks all conformal symmetries. We achieve this by using the resolvent method rather than standard CFT techniques, and derive closed expressions for the Rényi entropies, modular Hamiltonian and flow of the radiation. We determine the conditions under which mirrors generate unitary transformations, leading to Page curves resembling those expected from black hole evaporation. These results also yield the Rényi entropies on AdS₂ with reflecting asymptotic boundary conditions, which have applications to recent discussions of Hawking radiation. The results are ready to be used for a variety of applications in the field.

INTRODUCTION

Since a long time already it has been understood that the physics of moving mirrors in QFT is intimately connected – and in some cases exactly equivalent – to the thermodynamics of black holes. This relation has proven very fruitful, since the former does not require involved geometric considerations but rather only some fundamental notions about quantum fields.

Two main strategies have been traditionally used in this subject. The first one consists of computing the global properties of the asymptotic state – e.g. defined at future null infinity, and resembles more closely Hawking’s original calculation [1–9]. More recently techniques coming from gauge/gravity duality, specifically the Ryu-Takayanagi formula and its generalisations [10–12], allow to translate the problem into gravitational physics in a higher dimensional space [13–15]. This second approach relies strongly on methods of conformal field theory. And despite much progress, some important questions remain open.

Often the above approaches restrict to studies of entanglement entropy. However, a quantum state is not determined only by its entanglement entropy. What one would like to figure out is the structure of the density matrix itself as the system evolves. This means that we seek to understand the correlations between arbitrary *subsystems* of the radiation, a property that is neither global nor fixed by conformal symmetry.

In this work we do precisely this for a very simple system: the chiral fermion in 1 + 1–dimensions with a reflecting boundary. The advantage is that here we have the luxury of using the method of the resolvent [16].

Finding the Rényi entropies is particularly important

in connection with the information paradox. Indeed, requiring that the von Neumann entropy of the radiation follows a Page curve and returns to its original value is necessary but not sufficient to ensure unitarity. What is needed is that *all* Rényi entropies behave in this way. We will see under which conditions this is true for moving mirrors. Mutual information will help us quantify the correlations between the early radiation that has escaped and the later one that is close to perturbation region.

Here is an executive review of the main results. For moving mirrors in flat space the Rényi entropies of arbitrary regions are given in (38), with the explicit examples of a static and uniformly accelerating mirrors in (53) and (59). Mutual information between two subregions is given in (42) and plotted in fig. 4 comparing two different mirrors. The kernels of the modular Hamiltonian and flow are in (44) and (49), and the action of the modular operator in (51) and we illustrated it in fig. 2. The Rényi entropies for thermal states on AdS₂ are in (65). A more thorough application to black hole will be considered elsewhere.

FERMIONS AND MIRRORS.

We consider the standard massless Dirac action over a patch \mathcal{M} of 1 + 1-dimensional Minkowski spacetime. As usual, using lightcone coordinates $x^\pm = t \pm x$ this reads

$$I = \frac{i}{2} \int_{\mathcal{M}} dx dt \left(\psi_-^\dagger \partial_+ \psi_- + \psi_+^\dagger \partial_- \psi_+ \right) \quad (1)$$

where ψ_\pm are the two components of the Dirac spinor.

We are interested in the case when \mathcal{M} has a boundary $\partial\mathcal{M}$ along a worldline specified by a differentiable monotonically increasing function

$$x^+ = g(x^-) \quad (2)$$

*Electronic address: ignacio.reyes@aei.mpg.de

It is important to notice that since the mirror trajectory is subluminal, only the diagonal entries of \mathbf{G} have a pole for coinciding points measured at equal times,

$$G_{\pm\pm}(x \rightarrow y) \sim \pm \frac{1}{2\pi i(x-y)}. \quad (12)$$

This shows that the presence of the mirror does not modify the UV physics, and is relevant in our analysis below.

Our aim is to investigate the entanglement in the radiation generated by the mirror. We start by choosing an incoming state specific by (8) and a mirror trajectory specified by $g(\cdot)$. Together these determine some global state ρ_Σ on each Cauchy slice Σ , see fig. 1. We now choose a subregion $V \subset \Sigma$ consisting of N disjoint intervals $V = \cup_\ell (a_\ell, b_\ell)$ with $\ell = 1, \dots, N$, and wish to compute the reduced density matrix $\rho_V = \text{Tr}_{V^c}(\rho_\Sigma)$ obtained by tracing out the complement of V along Σ . [43]

Here is where having a free theory comes in handy [18]. For free fermions, it is sufficient that ρ_V reproduces the correlator on V

$$\mathbf{G}(x, y) = \text{tr}_V(\rho_V \Psi(x) \Psi^\dagger(y)) \quad , \quad x, y \in V. \quad (13)$$

Now any state can be written as

$$\rho_V = \frac{e^{-K_V}}{\text{Tr} e^{-K_V}} \quad (14)$$

where K is called the *modular Hamiltonian*. For gaussian states this takes a quadratic form

$$K = \int_{V^2} dx dy \Psi^\dagger(x) \mathbf{k}(x, y) \Psi(y) \quad (15)$$

with kernel [18]

$$\mathbf{k} = -\log(\mathbf{G}^{-1} - \mathbf{1}). \quad (16)$$

Here and below $\mathbf{G}(x, y)$ is taken as a linear operator acting on smooth functions supported on V via convolution ('matrix multiplication' in x, y).

The previous discussion has converted the problem of finding the reduced density matrix into that of computing functions of \mathbf{G} on a one-dimensional subspace V , but with both chiralities simultaneously. For simplicity we restrict to Cauchy slices of constant time, the generalisation being straightforward. This sets the stage for the application of the resolvent method.

RESOLVENT

This section contains the main technical tools of this work, following the approach of [19–21]. Given an operator \mathbf{G} of bounded spectrum and a function $f(\lambda)$ holomorphic in the interior of a contour γ enclosing the spectrum

– in the case of fermions, the interval $[0, 1]$ – Cauchy's integral formula defines the function of an operator by

$$f(\mathbf{G}) = \frac{1}{2\pi i} \oint_\gamma d\lambda \frac{f(\lambda)}{\lambda - \mathbf{G}}. \quad (17)$$

The challenge is of course to compute the operator $(\lambda - \mathbf{G})^{-1}$ known as the *resolvent*. Again, the boldface notation indicates that these are 2×2 matrices associated to the Dirac spinor. The resolvent possess a branch cut along the spectrum.

We proceed in two steps. First, we will reduce the spinorial integral equation into a more familiar one associated to a single chirality. Second, we recast the problem as a contour equation in the complex plane and solve it via residue analysis. We begin by a convenient change of variables,

$$\frac{1}{\lambda - \mathbf{G}} = \frac{1}{\lambda} + \frac{1}{\lambda^2} \mathbf{F} \quad (18)$$

which turns the functional equation $(\lambda - \mathbf{G}) \times (\lambda - \mathbf{G})^{-1} = \mathbf{1}$ into the integral equation

$$-\mathbf{G}(x, y) + \mathbf{F}(x, y) - \frac{1}{\lambda} \int_V dz \mathbf{G}(x, z) \mathbf{F}(z, y) = \mathbf{0}. \quad (19)$$

In order to solve this equation, we shall first propose an Ansatz for \mathbf{F} and transform this equation into a standard scalar integral equation. We propose a solution with a similar structure as \mathbf{G} itself:

$$F_{ij}(x, y) = \epsilon^{\frac{i-j}{2}} \sqrt{(-1)^{\frac{i-j}{2}}} q'_i(x) q'_j(y) F(q_i(x), q_j(y)). \quad (20)$$

With this Ansatz, a straightforward calculation shows that the singular integral equation becomes

$$-G(q_i, q_k) + F(q_i, q_k) - \frac{1}{\lambda} \int_V dz \quad (21)$$

$$[G(q_i, z^+) F(z^+, q_k) + g'(z^-) G(q_i, g(z^-)) F(g(z^-), q_k)] = 0. \quad (22)$$

Since by assumption $g(\cdot)$ is smooth and monotonically increasing, (22) can be recasted as a simpler integral equation

$$-G(x, y) + F(x, y) - \frac{1}{\lambda} \int_V dz G(x, z) F(z, y) = 0 \quad (23)$$

where now x, y belong to the region \tilde{V} defined by

$$\tilde{V} := V^+ \cup g(V^-) \quad (24)$$

where

$$V^+ = \cup_\ell (a_\ell^+, b_\ell^+) \quad , \quad g(V^-) = \cup_\ell (g(b_\ell^-), g(a_\ell^-))$$

The region \tilde{V} consists of the null 'reflections' of V through the mirror. Thus, we have effectively reduced

the spinorial problem on V on a semi-infinite line to a scalar problem on a different region \tilde{V} on the real line.

In [19] a recipe was provided to find the scalar function F that solves (23). The first step consists of rewriting the LHS of (23) as a contour integral in the complex plane,

$$\oint_{\tilde{V}} dz G(x, z) F(z, y) = 0, \quad (25)$$

while the second step is to solve the resulting equation via residues. For the first step, we require that in a neighbourhood of $\tilde{V} \subset \mathbb{C}$, F possesses:

- A single pole along \tilde{V}

$$F(z \rightarrow y, y) \sim \frac{1}{2\pi i(y-z)} + \dots \quad (26)$$

- A multiplicative branch cut along along the region,

$$F(z + i0^-, y) = \frac{\lambda - 1}{\lambda} F(z - i0^+, y), \quad z \in \tilde{V} \quad (27)$$

- Vanishing residues around $\partial\tilde{V}$, and analytic everywhere else in an neighbourhood of \tilde{V} .

As shown in [19], these requirements are sufficient to completely determine F for the class of states (8) considered here. The solution to (22) is

$$F_{ij}(x, z) = G_{ij}(x, z) \left(\frac{\lambda - 1}{\lambda} \right)^{i(Z(q_i(x)) - Z(q_j(z))) - 1}. \quad (28)$$

where

$$Z(x) = \frac{1}{2\pi} \log \Omega(x) \quad (29)$$

with

$$\Omega(x) = - \prod_{\ell} \frac{G(x, b_{\ell}^+) G(x, g(a_{\ell}^-))}{G(x, a_{\ell}^+) G(x, g(b_{\ell}^-))}. \quad (30)$$

The factor $G_{ij}(x, z)$ in (28) provides the pole required in (26). The function Z is the result of the desired branch cut (27) and depends on both the region and the propagator. Replaced back in (20) this gives the four components of \mathbf{F} which in turn provides the resolvent via (18). This concludes the construction of the resolvent.

A subtlety of how to obtain (28) is in order. Notice the extra factor of -1 in the exponent of (28). The reason for its presence the following. The solution to the contour equation with $x, y \in \mathbb{C}$ is (28) but without this factor. Then, one must take the limit $x + i0^{\pm}, y + i0^{\mp}$ to obtain the result on \tilde{V} . In doing so, the exponent acquires an extra factor due to the cut in λ , if we wish to express now both x and y on the same side of the cut. Once this limit is taken, (28) has no cuts along \tilde{V} , and provides the solution to the integral equation.

We finish this technical section by providing a useful formula. Replacing (18) back into (17), one finds

$$f(\mathbf{G}) = \frac{1}{2\pi i} \oint_{\gamma} d\lambda \frac{f(\lambda)}{\lambda^2} \mathbf{F} \quad (31)$$

where we dropped the first term in (18) since the associated integrand is holomorphic inside γ . Then, we can use the branch cut of \mathbf{F} in the variable λ in order to recast the contour integral as a regular integral over the spectrum. From (28) it is easy to see that F just above and below the cut along $\lambda \in [0, 1]$ satisfy

$$F_{jk}(x, y)|_{\lambda+i\epsilon} = \frac{\Omega(q_j(x))}{\Omega(q_k(y))} F_{jk}(x, y)|_{\lambda-i\epsilon}. \quad (32)$$

This yields the spectral decomposition of the correlator:

$$f(\mathbf{G})_{jk} = \frac{1}{2\pi i} \int_0^1 d\lambda \frac{f(\lambda)}{\lambda^2} \left[1 - \frac{\Omega(q_j(x))}{\Omega(q_k(y))} \right] F_{jk}|_{\lambda-i\epsilon}. \quad (33)$$

This formula is ready to be used for any desired function f holomorphic in the interior of γ . The simplest application is computing the Renyi entropies, to which we now turn.

ENTROPIES

The entanglement Rényi entropies are defined as

$$S^{(n)} = \frac{1}{1-n} \log \frac{\text{Tr}(\rho^n)}{(\text{Tr} \rho)^n}. \quad (34)$$

For the free fermion, it is easy to show that

$$\log \text{Tr}(\rho^n) = \text{Tr} \log(\mathbf{G}^n + (1 - \mathbf{G})^n). \quad (35)$$

To compute this we can use the spectral decomposition (33) replacing $f = \log(\lambda^n + (1 - \lambda)^n)$, taking the trace and performing the integral in λ . The trace is easy to compute since, due to the pole in the propagator, it yields a boundary term,

$$\text{Tr} \left[\left(1 - \frac{\Omega(q_{\pm}(x))}{\Omega(q_{\pm}(y))} \right) F_{\pm\pm} \right] = \pm \frac{i}{2\pi} \frac{\lambda}{\lambda - 1} \log \Omega(q_{\pm}(x)) \Big|_{\partial V}. \quad (36)$$

Replacing this into the spectral decomposition, all the λ -dependence is isolated into a prefactor given by [44]

$$\frac{1}{4\pi^2} \int_0^1 d\lambda \frac{\log(\lambda^n + (1 - \lambda)^n)}{\lambda(\lambda - 1)} = \frac{1 - n^2}{24n}. \quad (37)$$

The last step to obtain the entropies is to regularise their well known UV divergences. This is done by considering the region $V_{\delta} = \cup_{\ell} (a_{\ell} + \delta, b_{\ell} - \delta)$ with a very

small $\delta > 0$. Putting everything together, we arrive at the Rényi entropies,

$$S^{(n)} = \frac{n+1}{24n} \log \frac{\Omega(x^+)}{\Omega(g(x^-))} \Big|_{\partial V_\delta}. \quad (38)$$

This expression is quite general. It is valid for a causal and differentiable but otherwise arbitrary mirror trajectory parametrised by the function g . The entangling region V is also an arbitrary set of disjoint intervals. The incoming state from \mathcal{I}_R^- is a thermal ensemble at inverse temperature β . And just as in (38), throughout the paper all n -dependence of Rényi entropies appears as an overall factor. To get the entanglement entropy, just set $n \rightarrow 1$.

Here it is illustrative to look at a specific example. Consider the vacuum as incoming state and a single interval (a, b) at time t but leaving the mirror trajectory $g(\cdot)$ arbitrary. The entropies (38) yield

$$S^{(n)} = \frac{n+1}{12n} \log \left(\frac{b-a}{\delta^2} \frac{\frac{b^+ - g(b^-)}{b^+ - g(a^-)}}{\frac{a^+ - g(b^-)}{a^+ - g(a^-)}} \frac{g(a^-) - g(b^-)}{\sqrt{g'(b^-)g'(a^-)}} \right). \quad (39)$$

This result is remarkably simple and exhibits the unitarity feature alluded to in the beginning of the paper. For the same region and incoming state, two different mirror trajectories g_1 and g_2 will radiate differently and thus produce different reduced states $\rho_V[g_{1,2}(t)]$. However the Rényi entropies (39) – and therefore the entanglement spectrum – depend on the mirror only through its position and velocity at the null projection of the region's endpoints. We thus conclude that: *two mirrors with identical position and velocity at the null projections of ∂V generate reduced states related by a unitary transformation*

$$U \rho_V[g_1(t)] U^\dagger = \rho_V[g_2(t)]. \quad (40)$$

The behaviour of the mirror anywhere else along its history is irrelevant. Here it is crucial to observe that the states $\rho_V[g_{1,2}]$ can be arbitrarily different, as they depend on the behaviour of the mirror along the projection of V itself and not just its boundary. For example they can have different energy distributions. The point is that the resulting states have identical set of Rényi entropies. Notice also that this argument does not follow from the entropy of the complement being the same, as the incoming state needs not be pure.

An analogous statement holds when comparing the states produced by the same mirror but at different times. If the position and velocity of the mirror is the same at t_1 and t_2 , it is easy to see that all factors in (39) return to their original values thus implying

$$U \rho_V[g(t_1)] U^\dagger = \rho_V[g(t_2)]. \quad (41)$$

for some unitary U . This case is depicted in figure 1. This behaviour is what should be expected for black hole evaporation: not only the entanglement entropy but *all* Rényi entropies must coincide between the initial and final states.

At this point we must make a remark regarding the physical reality of this discussion. As is well known, Rényi entropies are not physical quantities since they suffer from UV divergences as $\delta \rightarrow 0$. In particular, the dependence of (39) on the mirror velocities is such a regularisation artefact. Thus, one might fear that the conclusions above lack physical significance. This is not the case: since the entropies take the form $\log(\alpha\delta^{-1} + \mathcal{O}(1))$ for some α as $\delta \rightarrow 0$, the subleading correction to the entropies vanishes in this limit. Therefore the results highlighted above regarding unitarity remain valid in the UV. This is different in higher dimensions.

A more robust physical insight is gained by considering quantities that are UV finite by construction. One such measure of entanglement is mutual information (MI), which involves two regions $V_{1,2}$, and is given by $I(V_1|V_2) = S^{(1)}(V_1) + S^{(1)}(V_2) - S^{(1)}(V_1 \cup V_2)$. Let's choose two disjoint intervals $V_1 = (a_1, b_1)$, $V_2 = (a_2, b_2)$ again at constant t like in fig. 1. From (38) we find that the mutual information in the presence of a moving mirror decomposes as

$$I = I_{\text{plane}} + \frac{1}{6} \log \omega. \quad (42)$$

Again let's consider the simple case of the vacuum as incoming state. The first term is the usual mutual information of two independent chiralities on the plane (no boundary), $I_{\text{plane}} = \frac{1}{6} \log \chi$ where $\chi = \frac{(a_2 - a_1)(b_2 - b_1)}{(b_2 - a_1)(a_2 - b_1)}$ is the cross ratio. The new contribution due to the mirror is parametrised by ω as

$$\omega = \frac{\frac{(b_2^+ - g(a_1^-))(b_1^+ - g(a_2^-))(g(b_2^-) - g(b_1^-))}{(b_2^+ - g(b_1^-))(b_1^+ - g(b_2^-))(g(b_2^-) - g(a_1^-))}}{\frac{(a_2^+ - g(a_1^-))(a_1^+ - g(a_2^-))(g(a_2^-) - g(b_1^-))}{(a_2^+ - g(b_1^-))(a_1^+ - g(b_2^-))(g(a_1^-) - g(a_2^-))}}, \quad (43)$$

with a similar expression holding for incoming thermal states. It is noteworthy that although the individual entropies depend on the mirror velocity, mutual information is independent of it. The velocity dependence arises via the UV divergences, which mutual information is devoid from by construction. We apply this result below in the examples.

MODULAR HAMILTONIAN AND FLOW

The modular Hamiltonian introduced in (14) plays an important role in many areas of physics such as algebraic QFT, topological order, tensor networks, relative entropy, energy conditions and bulk reconstruction [22–28]. As we saw above, for gaussian free fermion states

it takes the quadratic form (15) defined by the kernel (16). Once again the resolvent techniques described before provide the answer. In this case it is given as the contour integral

$$k_{ij} = \epsilon^{\frac{i-j}{2}} \sqrt{(-1)^{\frac{i-j}{2}} q'_i q'_j} G(q_i, q_j) \oint_{\gamma} d\lambda \frac{f(\lambda)}{\lambda(\lambda-1)} \left(\frac{\lambda}{\lambda-1} \right)^{i\tilde{t}}$$

where $f = -\log(\lambda^{-1} - 1)$, and we have abbreviated $q_i = q_i(x)$ and $\tilde{t} = Z(x) - Z(y)$. Contour integrals of this form have been evaluated in [19, 21]. The result is:

$$k_{ij}(x, y) = -2\pi\delta\left(Z(q_i(x)) - Z(q_j(y))\right) G_{ij}(x, y). \quad (44)$$

From this, two features stand out as characterising the modular Hamiltonian. First, the modular Hamiltonian couples both chiralities, since the kernel (44) is not diagonal: k_{ij} is the coupling between chiralities i and j . The second feature regards its locality. By *local* we mean that $k \propto \delta(x - y)$ so the modular Hamiltonian couples a point only to itself. *Bi-local* means that $k \propto \delta(x - f(y))$ for some function f , so that x is coupled only to a specific set of points y . *Completely-nonlocal* means k is a smooth function of two variables with support on V^2 .

Thus to understand the locality properties of (44), we must examine the number and nature of the solutions to

$$Z(q_i(x)) - Z(q_j(y)) = 0. \quad (45)$$

For our purposes only one property of the function $Z(\cdot)$ is relevant: $Z(q_i)$ for $i = \pm$ increases/decreases monotonically from $\pm\infty$ to $\mp\infty$ in each interval of V , regardless of the scattered state or the mirror trajectory. Therefore, there exists a unique solution to (45) in each interval as follows.

For equal chiralities, $i = j$, we call the solutions $y_\ell(x)$ where $\ell \in 1, \dots, N$ labels the interval. These are similar – but not identical – to those already encountered in [16, 21, 29, 30], and includes the *local* solution $y = x$. For opposite chiralities $i = -j$, we have a novel set of solutions which we call $y_{-\ell}$ to indicate that they are associated to a change in chirality. See fig. 2 for an example.

The modular Hamiltonian allows to define the *modular flow*, an automorphism $\sigma_t(\cdot)$ of the algebra of observables supported on the causal region associated to V . It is defined as conjugation with the modular Hamiltonian itself,

$$\sigma_\tau(\mathcal{O}) := e^{-i\tau K} \mathcal{O} e^{i\tau K} \quad (46)$$

The most natural flow to study is that of the fundamental field itself. It is given by [21]

$$\sigma_\tau(\psi_i(x)) = \int_V dy \Sigma_{ij}(x, y) \psi_j(y) \quad (47)$$

with the modular kernel

$$\Sigma = (\mathbf{G}^{-1} - 1)^{-i\tau}. \quad (48)$$

This kernel has a clear physical interpretation: Σ_{ij} is the rate at which the modular flow (46) converts the operator of chirality i into that of chirality j . And once more the resolvent computes this function elegantly; the result is

$$\Sigma_{ij} = 2\pi i \sinh(\pi\tau) \delta(Z(q_i(x)) - Z(q_j(x)) - \tau) G_{ij}(x, y). \quad (49)$$

Similarly to the modular Hamiltonian, Σ_{ij} is supported only on the solutions of

$$Z(q_i(x)) - Z(q_j(y)) - \tau = 0. \quad (50)$$

Introducing the kernel (49) into (47) yields the final formula for the modular flow. The modular flow is explicitly given by

$$\begin{aligned} \sigma_\tau(\psi_i(x)) = 2\pi \sinh(\pi\tau) \sum_\ell \left[\frac{G_{ii}(x, y_\ell(x)) \psi_i(y_\ell(x))}{|\partial_y Z(y) \partial_y q_i(y)|_{y=y_\ell(x)}} \right. \\ \left. + \frac{G_{i,-i}(x, y_{-\ell}(x)) \psi_{-i}(y_{-\ell}(x))}{|\partial_y Z(y) \partial_y q_{-i}(y)|_{y=y_{-\ell}(x)}} \right]. \quad (51) \end{aligned}$$

Modular flow takes the field of chirality i at point x , and evolves it to exactly two points on each interval: a contribution of the same chirality located at $y_\ell(x)$, and another with opposite chirality located at $y_{-\ell}(x)$. These points correspond to the solutions to (50) and are depicted in fig. 2 for the case of two intervals and a static boundary with the vacuum as incoming state.

Two general lessons stem out of the the analysis above regarding modular flow in the presence of mirrors. First: a boundary introduces additional non-localities as compared to the no-boundary case. These correspond to the components of modular flow that exchange chiralities. Second: the radiation created by a moving mirror cannot change qualitatively the locality properties of modular flow already present for the static boundary. For instance, it will not produce full non-locality out of bi-locality.

EXAMPLES OF MIRRORS.

All the discussion above applies to arbitrary mirror trajectories, provided they are causal and differentiable. In this section we consider specific examples which are of particular physical interest.

A static mirror (RHP)

As our simplest example, consider a single interval on the right half plane (RHP), i.e. a static boundary at $x = 0$ or $x^+ = x^-$. This does give rise to a conformal

boundary condition where (6) vanishes. For the vacuum as incoming state, the Rényi entropies (38) give

$$S_{\text{RHP}}^{(n)} = \frac{n+1}{12n} \left[\log \left(\frac{b-a}{\delta} \right)^2 + \log \frac{4r}{(r+1)^2} \right] \quad (52)$$

where $r = b/a$. These agree with those reported in [31] recently. The first term is simply twice the universal entropy of a single chirality, while the second one is due to the mirror. If the incoming state is thermal, the entropies are instead

$$S_{\text{RHP}}^{(n)} = \frac{n+1}{12n} \left[\log \left(\frac{\beta}{\pi\delta} \sinh \frac{\pi(b-a)}{\beta} \right)^2 + \log \frac{4\tilde{r}}{(\tilde{r}+1)^2} \right] \quad (53)$$

where $\tilde{r} = \tanh \frac{2\pi a}{\beta} / \tanh \frac{2\pi b}{\beta}$.

These results illustrate a fundamental property of entanglement. The second term in both (52) and (53) is always negative; thus for all static cases the mirror *lowers* the entropy of the system. This is a consequence of *monogamy of entanglement*: since the two chiralities are now entangled to each other, they cannot be as entangled with the rest of the system as in the no-boundary case in equilibrium [45]. This is important because it means that the entropies of the quantum correlated chiralities have a slower scaling with the ratio r (or \tilde{r}) than their uncorrelated counterparts. As we will see below, this has important consequences in two dimensional gravity.

Let us now consider the case of two intervals. The static mirror contribution to the mutual information (42) is parametrised by

$$\omega_{\text{RHP}} = \frac{\sinh \frac{\pi(a_1+b_2)}{\beta} \sinh \frac{\pi(a_2+b_1)}{\beta}}{\sinh \frac{\pi(a_1+a_2)}{\beta} \sinh \frac{\pi(b_1+b_2)}{\beta}} \quad (54)$$

which becomes $\frac{(a_2+b_1)(a_1+b_2)}{(a_1+a_2)(b_1+b_2)}$ at zero temperature. Let us now describe the modular flow for the vacuum. First, (30) reduces to

$$\Omega(x) = -\frac{(x-a_1)(x+b_1)(x-a_2)(x+b_2)}{(x-b_1)(x+a_1)(x-b_2)(x+a_2)} \quad (55)$$

Recall that eq. (50) determines which points are coupled along the flow. In this case (50) a quartic equation yielding four real solutions that we label $y_{\pm\ell}$ where \pm indicates the chirality of the contribution while $\ell = 1, 2$ labels the intervals. This is depicted in fig. 2. For more intervals, the situation is completely analogous, involving two points per interval.

From vacuum to thermal and back

One of the characteristic features of Hawking radiation is that the outgoing state measured at \mathcal{I}^+ is thermal. In

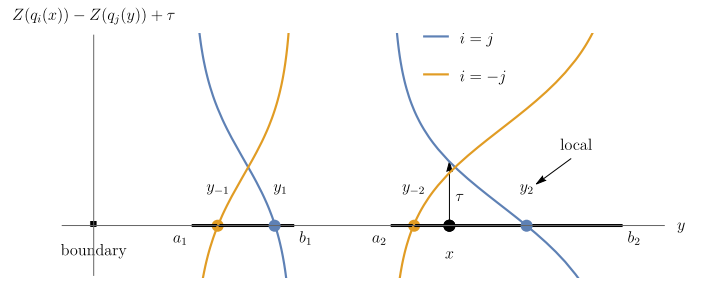


FIG. 2: Illustration of the modular evolution governed by (47), for two disjoint intervals and a static mirror. We plot (50), for equal and opposite chiralities (this is not a spacetime diagram). The modular flow of $\psi_i(x)$ yields, at each interval, contributions of both chiralities $\psi_{\pm i}$ located at the points $y_{\pm\ell}(x)$ that are solutions to (50) (coloured circles). Evolution in modular time τ shifts the curves vertically, and the roots evolve accordingly. The root at y_2 is the local (geometric) solution, with $y_2 \rightarrow x$ as $\tau \rightarrow 0$.

our moving mirror setup, there is a unique mirror profile that takes an incoming vacuum and renders the outgoing modes asymptotically in a thermal state at inverse temperature β . This is

$$g_{\text{I}}(x^-) = \frac{\beta}{\pi} \tanh \left(\frac{\pi}{\beta} x^- \right) \quad \text{vacuum} \rightarrow \text{thermal} \quad (56)$$

This can only hold in the asymptotic future – indeed the trajectory (56) becomes null also in the remote past producing singularities, so this early stage must be replaced by a timelike one as we have mentioned above, see fig. 3. Interestingly the converse effect is also possible: given an incoming thermal state, any trajectory that asymptotes to the inverse function, namely

$$\tilde{g}_{\text{I}}(x^-) = \frac{\beta}{\pi} \operatorname{arctanh} \left(\frac{\pi}{\beta} x^- \right) \quad \text{thermal} \rightarrow \text{vacuum} \quad (57)$$

takes a thermal state and reflects it as the vacuum. Of course this is only defined up to its intersection with \mathcal{I}_R^+ .

These are good examples of the breaking of conformal symmetry. The energy flux flowing away from the system (6) gives

$$\langle : T_{\parallel\perp} : \rangle |_{\text{mirror}} = \begin{cases} -\frac{\pi \cos^2(\pi x^-/\beta)}{6\beta^2} < 0 & g_{\text{I}} \\ \frac{\pi}{6\beta^2 - \pi^2(x^-)^2} > 0 & \tilde{g}_{\text{I}} \end{cases}$$

indicating that positive energy is injected to form the thermal state from the vacuum, while the converse is true for the opposite case. We avoid writing the entropies explicitly here but these can be obtained directly by replacing (56) into (38) appropriately. Next we will consider one last example before turning to the problem of how to obtain a physical Page curve.

Uniform acceleration

An important example is a mirror moving with constant proper acceleration. The mirror stands static at $x = -R$ until $t = 0$ when it begins to accelerate at constant rate away from the physical region, following the trajectory $t^2 - x^2 = x^+ x^- = -R^2$ corresponding to

$$g_{\text{III}}(x^-) = -R^2/x^- . \quad (58)$$

Although qualitatively this profile is similar to g_{I} , it exhibits some interesting features absent in that case. Since we already know the static history, let us take as an example a single region that is completely contained in the future of the accelerated portion of the trajectory, e.g. V_1 in fig. 3. The Rényi entropies as a function of time read (for $t > b - R$)

$$S^{(n)} = \frac{n+1}{12n} \left[\log \left(\frac{b-a}{\delta} \right)^2 + \log \frac{(t^2 + R^2 - a^2)(t^2 + R^2 - b^2)}{t^4 - t^2(a^2 + b^2 - 2R^2) - (R^2 - ab)^2} \right] . \quad (59)$$

This result displays an interesting feature. Notice the first term is identical to the vacuum Rényi entropy of *two* independent chiralities, as if the mirror was not present. In the limit of very large times, the second term vanishes. This indicates that the original entanglement between the two chiralities, created by the static mirror, is ‘erased’ by the accelerating mirror. This is indeed the case and can be seen directly by looking back at the correlation matrix itself. It is easy to show that in the limit $t \rightarrow \infty$

$$G_{\pm\mp} \rightarrow 0 \quad \text{for } g_{\text{III}} \quad (60)$$

so that the correlations between left and right movers vanish. Because opposite chiralities are not entangled with each other any more on V , they become more entangled with the complement which has the effect of *increasing* the entropy. This is a hallmark of non-unitarity: the entropy of any region in the distant future is larger than its counterpart in the remote past.

Page curves from Mutual Information

Now we will show how to obtain Page curves for the correlations between the early radiation that has escaped far away, and the later radiation that is still close to the perturbing region. Consider two disjoint regions $V_\ell = (a_\ell, b_\ell)$, $\ell = 1, 2$ at fixed spatial positions. We will compare two trajectories that remain static until $t = 0$, when they begin to move. The first is g_{I} , already introduced, which scatters the vacuum into a thermal outgoing state. The second, g_{II} , follows g_{I} for some time but then deviates from it in order to smoothly return to the

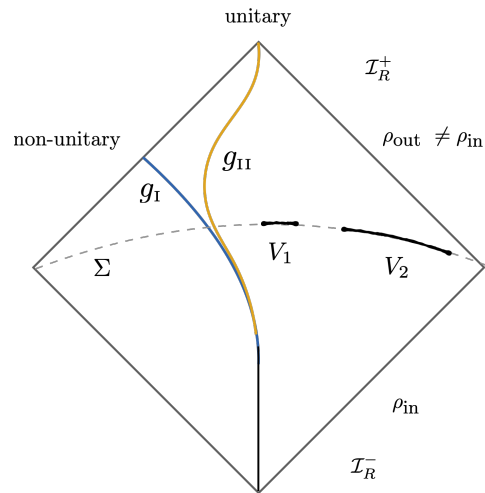


FIG. 3: Conformal diagram of flat space with different mirror trajectories, depicting an example with entangling region $V = V_1 \cup V_2$ whose entropies and modular flow we determine. Although the incoming and outgoing states $\rho_{\text{in/out}}$ are in general very different, unitarity means that their Rényi entropies on arbitrary regions match. This example illustrates g_{I} and g_{II} from the main text: the former starts to accelerate becoming asymptotically null, describing a non-unitary process. The latter follows the former for some time before returning to its original trajectory and respects unitarity.

static path. The precise functional form of g_{II} is irrelevant. See fig. 3.

In principle one could simply track the entropies of these regions of space as they evolve in time as done above. However, this approach is not completely satisfactory. First, Rényi entropies are not well defined in the UV since they contain divergences. Moreover, if we wish to keep track of *all* the radiation that has escaped to infinity, we must consider an unbounded spatial subregion, which introduces yet another divergence.

These problems are remedied by considering mutual information instead. MI is always finite: it is by construction free from UV divergences, and in addition we can safely take the limit $b_2 \rightarrow \infty$ that stretches all the way to spatial infinity. Furthermore, MI the natural physical interpretation that we seek: it measures the correlations between the early radiation (collected in V_2) and the late radiation (contained in V_1), a very relevant notion in the context of black holes.

In fig. 4 we plot the evolution of the MI between the early and late radiation as a function of time. Clearly for the trajectory g_{I} , there is a loss of correlations between the late and early radiation compared to trajectory g_{II} , which is unitary. The asymptotic difference in MI can be used to quantify this deviation from unitarity. In this

case, it is easy to compute from (43) and reads

$$\begin{aligned} \Delta I &= \lim_{t \rightarrow \infty} \lim_{b_2 \rightarrow \infty} (I_{g_{\text{II}}}(V_1|V_2) - I_{g_{\text{I}}}(V_1|V_2)) \\ &= \frac{1}{3} \log \frac{(a_2 - a_1)(a_2 + b_1)^2 \left(e^{\frac{2\pi a_2}{\beta}} - e^{\frac{2\pi b_1}{\beta}} \right)}{(a_2 - b_1)(a_1 + a_2)^2 \left(e^{\frac{2\pi a_2}{\beta}} - e^{\frac{2\pi a_1}{\beta}} \right)}. \end{aligned} \quad (61)$$

This measures the violation of unitarity as a function of the temperature of the outgoing radiation. It increases monotonically until saturating at high temperature. It does not vanish for zero temperature because we took the limit of late times first.

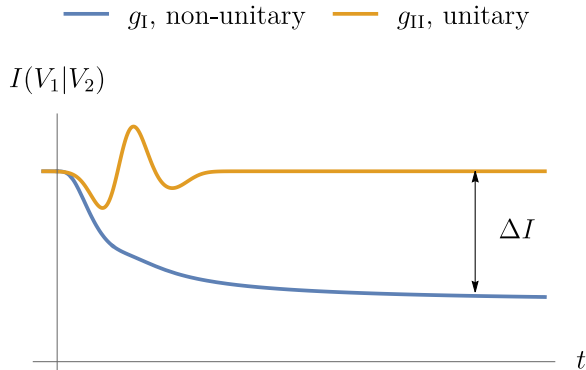


FIG. 4: Evolution of mutual information (42) between the regions V_1 and V_2 , for the two mirror trajectories depicted in fig. 3, measuring the amount of correlations between the early and late radiation. MI returns to its original value for trajectory g_{II} , whereas it doesn't for g_{I} , reflecting the underlying unitarity and non-unitarity respectively. The loss of correlations ΔI given in (61) serves to quantify unitarity violation.

BULK FIELDS ON AdS_2

The generalisation of all the above methods to curved backgrounds goes beyond the scope of this work and will be addressed in a forthcoming work [32]. Nevertheless, one can still obtain novel results on curved space by appropriately using the expressions derived above. The most direct application involves two dimensional anti-de Sitter space, whose metric in the Poincare patch is

$$ds^2 = \Lambda(x)^2(-dt^2 + dx^2) \quad (62)$$

with $\Lambda(x) = L/x$. The line $x = 0$ is a (static) asymptotic conformal boundary, which light rays reach at a finite coordinate time. Thus one must specify what happens at the boundary in order to fix the physics in the bulk.

A natural choice is to impose reflecting conditions at the asymptotic boundary. As mentioned above, a static boundary allows conformal boundary conditions, so that no energy leaks in or out of AdS. From the bulk perspective, this is indistinguishable from having the interior in

a thermal state in equilibrium with a reservoir and corresponds to the analogue of the state considered in [33]. The important point here is that AdS_2 is not conformally equivalent to the plane but the half plane. Luckily we have already solved the latter system above.

Following the standard replica construction [34], the traces of the reduced state ρ_V are given by the correlator of twist operators \mathcal{T} located at the endpoints:

$$\text{Tr}(\rho_V^n)|_{\text{AdS}_2} = \prod_r \langle \mathcal{T}(a_\ell) \tilde{\mathcal{T}}(b_\ell) \rangle_{\text{AdS}_2}. \quad (63)$$

Since the twist fields are primary with conformal weight $d_n = \frac{c}{12} \left(n - \frac{1}{n} \right)$ with c the Virasoro central charge, the Weyl rescaling that takes the right half plane into AdS_2 implies that

$$\text{Tr}(\rho_V^n)|_{\text{AdS}_2} = \text{Tr}(\rho_V^n)|_{\text{RHP}} \times \prod_\ell (\Lambda(a_\ell) \Lambda(b_\ell))^{-d_n}. \quad (64)$$

In consequence the Rényi entropies for Poincare AdS_2 with reflecting boundary conditions are

$$S_{\text{AdS}_2}^{(n)} = S_{\text{RHP}}^{(n)} + \frac{n+1}{12n} \log \prod_\ell \frac{L^2}{a_\ell b_\ell} \quad (65)$$

where the first term on the right corresponds to the entropies for the static mirror in flat space, either (53) at finite temperature or (52) for the vacuum, and we used $c = 1$ due to both chiralities.

For example, the entropy of a single interval (a, b) on the AdS_2 vacuum is

$$S_{\text{AdS}_2}^{(n)} = \frac{n+1}{12n} \log \left(\frac{2L}{\delta} \frac{r-1}{r+1} \right)^2. \quad (66)$$

The result depends only on the ratio $r = b/a$, as it should, given the scaling symmetry of the metric on a constant time slice, a feature not present in the flat space result (52). This is possible because AdS brings in a new scale – the curvature radius L – that compensates the dimensions of the UV cutoff δ . Moreover this simple case exemplifies that the entropies of a system of infinite extension need not be divergent, as can be seen from the limit $r \rightarrow \infty$ of (66).

Modular Hamiltonian and flow. We conclude here by observing that the previous arguments to obtain the AdS result in terms of the half plane do not apply for the modular Hamiltonian or flow. The reason is that the modular Hamiltonian (15) doesn't transform by a scaling under Weyl transformations: although the fields Ψ do, the kernel $\mathbf{k} = -\log(\mathbf{G}^{-1} - 1)$ in (16) doesn't. In other words, the naive replacement suggested by conformal symmetry doesn't solve the equation for the resolvent on AdS. This holds even for a single chirality. Thus, bulk modular Hamiltonian and flow for fermions on AdS_2 are not determined by their Minkowski counterparts but must be computed from first principles.

Application: Quantum extremal surfaces

Entanglement entropy has become a prominent topic in gauge/gravity duality mainly due to the Ryu-Takayanagi formula and its extensions [10–12]. This is a generalisation of the Bekenstein-Hawking law, stating that the *generalised* entropy of the dual field theory is given by

$$S_{\text{gen}} = \frac{A}{4G} + S_{\text{bulk}}. \quad (67)$$

Here A is the area of a codimension-2 surface in AdS anchored at the asymptotic subregion, whereas the second term is the bulk entanglement entropy of the fields bounded between the subregion and that surface. A *quantum extremal surface* (QES) [35] is the minimum of the variational principle $\delta S_{\text{gen}} = 0$. The results reported above find immediate applications in this context because they allow us to compute the second term of (67).

We consider AdS₂ black hole solutions of two-dimensional Jackiw-Teitelboim gravity [36–38] following the conventions of [39]. Here, the area term in (67) is replaced by the dilaton field ϕ which measures the area of the sphere of a higher-dimensional nearly extremal black hole. The solution for the dilaton in the coordinates (62) is

$$\phi(x) = \phi_0 + \frac{\phi_r}{x} \quad (68)$$

where ϕ_r is a positive constant and the second term comes from the area at extremality and is not important here. On top of this background, we place the fermions at zero temperature with reflecting boundary conditions.

From the holographic perspective it is natural to take one endpoint to the conformal boundary first, $a \rightarrow \delta$, since the RT surface is anchored there, and let the endpoint on b vary. However as pointed out earlier, the entropy $S_{\text{AdS}_2}^{(1)}$ becomes a constant in this limit! Thus, the QES would require to extremise

$$S_{\text{gen}} = \phi(b) + \frac{1}{3} \log \left(\frac{2L}{\delta} \right) + \mathcal{O}(\delta) \quad (69)$$

and since $\phi(x)$ is monotonic,

$$\partial_b S_{\text{gen}} = 0 \rightarrow \text{no solution}. \quad (70)$$

In other words, for fermions with asymptotic reflecting boundary conditions, there is no non-trivial quantum extremal surface in the zero temperature solution of JT gravity (we have excluded the solution $b \rightarrow \infty$ which corresponds to the horizon).

Let us see how these results differ from those in encountered in recent literature [39–42]. (Notice our conventions for the endpoints are somewhat reversed with respect to these; in order to compare we must replace $b \rightarrow a$ in our

expressions, and then take (5) of [40] in the limit $b \rightarrow 0$). Why do we get different results? First, these works have attached the boundary of AdS to a Minkowski region acting as a bath, via transparent boundary conditions. This is not essential for one can always trace out the bath, for example by reducing the density matrix on regions contained within the AdS side. More importantly, the states considered in these approaches and ours are different. We have considered the case where there are quantum correlations between the ingoing and outgoing fields, $G_{\pm} \neq 0$, whereas these works have considered states where the two opposite chiralities are in a product state, $G_{\pm} = 0$, but put at the same temperature so that the correlations between them are classical.

Not all observables are sensitive to distinguish these two states. For example, the local energy density of the two states is zero, so it is not enough to specify the energy in order to specify the state. However as we have discussed the entanglement entropy does. If instead of reflecting boundary conditions we simply consider two decoupled chiralities on AdS, the entropy of a single interval is determined by conformal symmetry; it is not given by (66) but rather

$$\tilde{S} = \frac{1}{6} \log \left(\frac{L}{\delta} \right)^2 \frac{(r-1)^2}{r} \quad \text{decoupled}. \quad (71)$$

Then, the associated generalised entropy $\tilde{S}_{\text{gen}} = \phi(x) + \tilde{S}$ gives

$$\partial_b \tilde{S}_{\text{gen}} = 0 \rightarrow b = 6\phi_r \quad (72)$$

This is the result obtained in [40] (again after sending the endpoint on the bath to the AdS boundary).

While both entropies are scale invariant, the entropies in the present work are always *lower* due to the monogamy of entanglement between the two chiralities. Because this arises from quantum correlations, its effect is most noticeable at low temperature. At high temperatures (black holes away from extremality) thermal correlations dominate, entanglement entropy becomes extensive, and the two different states considered give perturbatively similar results.

ACKNOWLEDGMENTS

It is a pleasure to thank Ana Alonso-Serrano, Enrico Brehm, Pedro F. Ramirez and the GQFI group at AEI for stimulating discussions. In particular I wish to thank Raúl Arias and Rob Myers for insightful comments on an early version of the draft. Specially I would like to thank Pascal Fries for joining the initial stages of the project as well as elucidating some subtle aspects. The Gravity, Quantum Fields and Information group at AEI is generously supported by the Alexander von Humboldt

Foundation and the Federal Ministry for Education and Research through the Sofja Kovalevskaja Award.

-
- [1] S. W. Hawking, “Black hole explosions,” *Nature*, vol. 248, pp. 30–31, 1974.
- [2] P. C. W. Davies and S. A. Fulling, “Radiation from a moving mirror in two-dimensional space-time conformal anomaly,” *Proc. Roy. Soc. Lond. A*, vol. 348, pp. 393–414, 1976.
- [3] P. C. W. Davies and S. A. Fulling, “Radiation from Moving Mirrors and from Black Holes,” *Proc. Roy. Soc. Lond. A*, vol. 356, pp. 237–257, 1977.
- [4] L. H. Ford and A. Vilenkin, “QUANTUM RADIATION BY MOVING MIRRORS,” *Phys. Rev. D*, vol. 25, p. 2569, 1982.
- [5] N. Tuning and H. L. Verlinde, “Back reaction on moving mirrors and black hole radiation,” 5 1996.
- [6] P. Chen and D.-h. Yeom, “Entropy evolution of moving mirrors and the information loss problem,” *Phys. Rev. D*, vol. 96, no. 2, p. 025016, 2017.
- [7] M. R. R. Good, E. V. Linder, and F. Wilczek, “Moving mirror model for quasithermal radiation fields,” *Phys. Rev. D*, vol. 101, no. 2, p. 025012, 2020.
- [8] M. R. R. Good, K. Yelshibekov, and Y. C. Ong, “On Horizonless Temperature with an Accelerating Mirror,” *JHEP*, vol. 03, p. 013, 2017.
- [9] M. Hotta, M. Shino, and M. Yoshimura, “Moving mirror model of Hawking evaporation,” *Prog. Theor. Phys.*, vol. 91, pp. 839–870, 1994.
- [10] S. Ryu and T. Takayanagi, “Holographic derivation of entanglement entropy from AdS/CFT,” *Phys. Rev. Lett.*, vol. 96, p. 181602, 2006.
- [11] V. E. Hubeny, M. Rangamani, and T. Takayanagi, “A Covariant holographic entanglement entropy proposal,” *JHEP*, vol. 07, p. 062, 2007.
- [12] T. Faulkner, A. Lewkowycz, and J. Maldacena, “Quantum corrections to holographic entanglement entropy,” *JHEP*, vol. 11, p. 074, 2013.
- [13] A. Almheiri, N. Engelhardt, D. Marolf, and H. Maxfield, “The entropy of bulk quantum fields and the entanglement wedge of an evaporating black hole,” *JHEP*, vol. 12, p. 063, 2019.
- [14] A. Almheiri, R. Mahajan, J. Maldacena, and Y. Zhao, “The Page curve of Hawking radiation from semiclassical geometry,” *JHEP*, vol. 03, p. 149, 2020.
- [15] I. Akal, Y. Kusuki, N. Shiba, T. Takayanagi, and Z. Wei, “Entanglement Entropy in a Holographic Moving Mirror and the Page Curve,” *Phys. Rev. Lett.*, vol. 126, no. 6, p. 061604, 2021.
- [16] H. Casini and M. Huerta, “Reduced density matrix and internal dynamics for multicomponent regions,” *Class. Quant. Grav.*, vol. 26, p. 185005, 2009.
- [17] J. L. Cardy, “Boundary conformal field theory,” 11 2004.
- [18] I. Peschel, “Calculation of reduced density matrices from correlation functions,” *Journal of Physics A: Mathematical and General*, vol. 36, pp. L205–L208, mar 2003.
- [19] P. Fries and I. A. Reyes, “Entanglement Spectrum of Chiral Fermions on the Torus,” *Phys. Rev. Lett.*, vol. 123, no. 21, p. 211603, 2019.
- [20] R. E. Arias, H. Casini, M. Huerta, and D. Pontello, “Entropy and modular Hamiltonian for a free chiral scalar in two intervals,” *Phys. Rev. D*, vol. 98, no. 12, p. 125008, 2018.
- [21] J. Erdmenger, P. Fries, I. A. Reyes, and C. P. Simon, “Resolving modular flow: a toolkit for free fermions,” 8 2020.
- [22] R. Haag, *Local quantum physics: Fields, particles, algebras*. Texts and monographs in physics, Berlin, Germany: Springer, 1992.
- [23] H. Li and F. D. M. Haldane, “Entanglement Spectrum as a Generalization of Entanglement Entropy: Identification of Topological Order in Non-Abelian Fractional Quantum Hall Effect States,” *Phys. Rev. Lett.*, vol. 101, p. 010504, Jul 2008.
- [24] D. D. Blanco and H. Casini, “Localization of Negative Energy and the Bekenstein Bound,” *Phys. Rev. Lett.*, vol. 111, no. 22, p. 221601, 2013.
- [25] L. Vanderstraeten, M. Mariën, J. Haegeman, N. Schuch, J. Vidal, and F. Verstraete, “Bridging perturbative expansions with tensor networks,” *Phys. Rev. Lett.*, vol. 119, p. 070401, Aug 2017.
- [26] H. Casini, M. Huerta, and R. C. Myers, “Towards a derivation of holographic entanglement entropy,” *JHEP*, vol. 05, p. 036, 2011.
- [27] D. L. Jafferis, A. Lewkowycz, J. Maldacena, and S. J. Suh, “Relative entropy equals bulk relative entropy,” *JHEP*, vol. 06, p. 004, 2016.
- [28] J. Cardy and E. Tonni, “Entanglement hamiltonians in two-dimensional conformal field theory,” *J. Stat. Mech.*, vol. 1612, no. 12, p. 123103, 2016.
- [29] I. Klich, D. Vaman, and G. Wong, “Entanglement Hamiltonians and entropy in 1+1D chiral fermion systems,” *Phys. Rev. B*, vol. 98, p. 035134, 2018.
- [30] D. Blanco and G. Pérez-Nadal, “Modular Hamiltonian of a chiral fermion on the torus,” *Phys. Rev. D*, vol. 100, no. 2, p. 025003, 2019.
- [31] M. Mintchev and E. Tonni, “Modular Hamiltonians for the massless Dirac field in the presence of a boundary,” 12 2020.
- [32] I. A. Reyes, “*in preparation*,”
- [33] S. W. Hawking and D. N. Page, “Thermodynamics of Black Holes in anti-De Sitter Space,” *Commun. Math. Phys.*, vol. 87, p. 577, 1983.
- [34] P. Calabrese and J. L. Cardy, “Entanglement entropy and quantum field theory,” *J. Stat. Mech.*, vol. 0406, p. P06002, 2004.
- [35] N. Engelhardt and A. C. Wall, “Quantum Extremal Surfaces: Holographic Entanglement Entropy beyond the Classical Regime,” *JHEP*, vol. 01, p. 073, 2015.
- [36] C. Teitelboim, “Gravitation and Hamiltonian Structure in Two Space-Time Dimensions,” *Phys. Lett. B*, vol. 126, pp. 41–45, 1983.
- [37] R. Jackiw, “Lower Dimensional Gravity,” *Nucl. Phys. B*, vol. 252, pp. 343–356, 1985.
- [38] J. Maldacena, D. Stanford, and Z. Yang, “Conformal symmetry and its breaking in two dimensional Nearly Anti-de-Sitter space,” *PTEP*, vol. 2016, no. 12, p. 12C104, 2016.
- [39] A. Almheiri, T. Hartman, J. Maldacena, E. Shaghoulian, and A. Tajdini, “Replica Wormholes and the Entropy of Hawking Radiation,” *JHEP*, vol. 05, p. 013, 2020.
- [40] A. Almheiri, R. Mahajan, and J. Maldacena, “Islands outside the horizon,” 10 2019.
- [41] T. Anegawa and N. Iizuka, “Notes on islands in asymp-

- totically flat 2d dilaton black holes,” *JHEP*, vol. 07, p. 036, 2020.
- [42] T. J. Hollowood, S. Prem Kumar, and A. Legramandi, “Hawking radiation correlations of evaporating black holes in JT gravity,” *J. Phys. A*, vol. 53, no. 47, p. 475401, 2020.
- [43] In the continuum limit the existence of the density operator is of course problematic. In this paper we abuse notation and use this notation since it is the more familiar language.
- [44] We thank Pascal Fries for a beautiful derivation of this formula.
- [45] We thank Pascal Fries for pointing out this interpretation.